

Protocrystalline Silicon at High Rate from Undiluted Silane

R.E.I. Schropp, M.K. van Veen, C.H.M. van der Werf, D.L. Williamson*, A.H. Mahan**
Utrecht University, Debye Institute, SID - Physics of Devices, P.O. Box 80000,
3508 TA Utrecht, The Netherlands

*Department of Physics, Colorado School of Mines, Golden, CO 80401

**National Renewable Energy Laboratory, Golden, CO 80401

ABSTRACT

Hot Wire Chemical Vapor Deposition (HWCVD) is shown to be a fast method for the deposition of protocrystalline silicon films from *undiluted* silane. Intrinsic silicon-hydrogen films (2 μm thick) have been deposited by HWCVD on plain stainless steel as well as on stainless steel precoated with a *n*-type doped microcrystalline silicon layer. In X-ray diffraction experiments, the linewidths of the first sharp peak (FSP) were 5.59 ± 0.09 degrees and 5.29 ± 0.11 degrees, respectively, indicating improved medium-range order and a template effect due to the $\mu\text{c-Si:H}$ *n*-layer. For thinner layers (0.7 μm thick), the linewidths of the FSP were 5.29 ± 0.09 degrees and 5.10 ± 0.09 degrees. These FSPs are as narrow as for optimized *i*-layers made by H_2 -diluted plasma deposition, however, at a much higher deposition rate (1 nm/s), at moderate temperature (250 °C), and without the use of H_2 dilution. In accompanying transmission electron micrographs, the layers show a significant concentration of elongated small voids in the growth direction that are not interconnected. Small Angle X-ray Scattering (SAXS) results are consistent with these observations. We suspect that the void nature allows the bulk of the film to be more ordered. The utilization of such layers in *n-i-p* solar cells on plain stainless steel leads to cells with a remarkably good stability, showing a decrease of the fill factor of less than 10 % during 1500 h of light soaking.

INTRODUCTION

During the last 10 years, technological and scientific developments are providing improved control of parameters in Hot Wire Chemical Vapor Deposition [1] (also called Catalytic Chemical Vapor Deposition (Cat-CVD; [2]). It is becoming clear that the deposition regime is fundamentally different from conventional Plasma Enhanced Chemical Vapor Deposition (PECVD). The high deposition rate of silicon-based thin films makes this method particularly interesting for application to, among others, low cost photovoltaic devices (solar cells) and thin film transistors (TFTs). For application of *a-Si:H* in these devices it is important to secure enhanced stability of the device characteristics (solar cell performance and the threshold voltage of thin film transistors) by using a material with an enhanced network ordering or so called protocrystalline silicon, for this material has been shown to possess higher stability against defect creation as due to the Staebler-Wronski effect [3].

In PECVD, as hydrogen dilution of the silane feedstock gas is necessary to produce protocrystalline silicon [4], it has not been possible thus far to reach a high deposition rate for such material. A typical deposition rate is 1 Å/s, and thus far to our knowledge, it has not become feasible to reach deposition rates higher than 3 Å/s using conventional PECVD. In

addition, the deposition parameters for achieving a protocrystalline regime are dependent on the type of substrate as well as film thickness dependent [5,6].

Previously, HWCVD has been shown to be capable of producing stable a-Si:H films with enhanced medium range order (MRO) [7]. The deposition rate for these films was already high (5-8 Å/s), but a possible drawback may be the high substrate temperature regime (360-425 °C) in which the materials were obtained. X-ray diffraction measurements indicated that the most stable materials exhibited the narrowest widths of the first scattering peaks (FSPs).

As the type of substrate has an influence on the degree of ordering in the deposited films, it has further been determined that PECVD conditions leading to *protocrystalline* silicon on n^+ -type doped layers lead to *microcrystalline* silicon on plain stainless steel [8]. Such substrate-dependent effects were also observed for the HWCVD layers, but only in the substrate temperature domain of 360-425 °C, instead of the 300 °C as used for PECVD experiments by Guha *et al.* [8]. Thus far, it was thought that for hot-wire deposited material either high substrate temperature or low bonded hydrogen content is needed to obtain protocrystalline material and there has been no evidence for the capability of HWCVD to produce protocrystalline silicon at low temperatures, similar to those used in PECVD. In this paper, we report for the first time on protocrystalline Si:H materials fabricated by HWCVD at relatively low substrate temperature (250 °C). Moreover, materials with protocrystalline characteristics were achieved in a high deposition rate regime (~ 10 Å/s) and without any H_2 dilution.

EXPERIMENTAL

The deposition equipment used in this study consists of two HWCVD chambers that are connected to a multichamber ultrahigh vacuum (UHV) system that has an additional 3 PECVD chambers. This arrangement offers the opportunity to create different geometries and deposition parameters that are optimized for each type of intrinsic layer (amorphous/proto/microcrystalline or polycrystalline). Tantalum filaments are used for deposition a-Si:H, proto-Si:H, and μ c-Si:H and substrate temperatures can be varied between 220 °C and 430 °C. With the help of a heat transport model [9] the substrate temperature has been carefully calibrated. The gas flow in the

HWCVD chambers is perpendicular to the length of the wires. The temperature of the wires is typically 1800 – 2000 °C. The substrate loading system is equipped with a shutter, which hermetically shields the substrate from any deposition during preheating.

The intrinsic layers made for the present investigations were all made from undiluted silane at 250 °C and 0.02 mbar. To investigate whether there is any ‘template’ effect on the

Table I. Sample identification in this study

Sample No.	Layer structure
1-Al	a-Si:H (2 μ m-intrinsic)/Al
1-SS	a-Si:H (2 μ m-intrinsic)/SS
2-Al	a-Si:H (2 μ m-intrinsic)/a-Si:H(50 nm-n-layer)/Al
2-SS	a-Si:H (2 μ m-intrinsic)/a-Si:H(50 nm-n-layer)/SS
3-Al	a-Si:H (2 μ m-intrinsic)/ μ c-Si:H(80 nm-n-layer)/Al
3-SS	a-Si:H (2 μ m-intrinsic)/ μ c-Si:H(80 nm-n-layer)/SS
1-SS'	a-Si:H (0.7 μ m-intrinsic)/SS
3-SS'	a-Si:H (0.7 μ m-intrinsic)/ μ c-Si:H (80 nm-n-layer)/SS

structure of the deposited films, we used substrates that were coated with a-Si:H or $\mu\text{c-Si:H}$ n-type layers (as in n-i-p solar cells) in addition to bare metal substrates.

As a sensitive tool for demonstrating protocrystallinity, we determine the peak width of the first scattering peak (FSP) in X-ray diffraction experiments (XRD). This method is in greater detail explained in a review paper [10]. As the samples 1-SS' and 3-SS' are rather thin (their thickness is closer to the i-layer thickness in n-i-p cells), long scan times of about 12 hours were used and each film was run twice to ensure reproducibility. Also, the back of the stainless steel substrate was scanned in order to allow subtraction of the substrate signal.

As further means for the characterization of this type of protocrystalline silicon, we used Small Angle X-ray Scattering (SAXS), Transmission Electron Microscopy (TEM), Fourier Transform InfraRed Spectroscopy (FTIR), and the flotation density technique (summarized in [11]). To allow SAXS measurements, stainless steel (SS) substrates were combined with Al foil substrates (10 μm thick, 99.999 % purity) were used. For the flotation density determinations, the same films on Al foil were used. Cross-sectional TEM and FTIR results were obtained using earlier samples made under the same conditions. For TEM, a glass substrate with an 80 nm $\mu\text{c-Si:H}$ n-type layer was used. For FTIR, polished highly resistive ($\sim 20 \text{ } \Omega\text{cm}$), p-type crystalline silicon wafer substrates with (100) orientation were used.

We also prepared n-i-p solar cells on plain SS, using 80 nm $\mu\text{c-Si:H}$ n-layers, intrinsic silicon layers (400 nm thick) made under the same conditions, and 20 nm $\mu\text{c-Si:H}$ p-layers. These cells were provided with an 80 nm thick ITO contact and Ag or Au grid structure. After recording the initial J-V curves, these cells were light soaked to determine their stability using an illumination intensity of 1 sun while keeping the sample temperature at around 45 °C. The evolution of the FF was recorded.

RESULTS

Fig. 1 shows the XRD data after subtraction of the SS substrate using the procedure as in [10]. These patterns were computer fitted to obtain quantitative values of the full-width-at-half-maximum (FWHM) and position (P) of the first sharp peak (FSP) of the intrinsic a-Si:H layer [2]. Also the thinner layers on SS in Table 1 were measured. Table 2 lists the quantitative results from all fits. In all cases where a $\mu\text{c-Si:H}$ n-layer was present, the integrated intensities of the (111), (220), and (311) peaks amounted to a fraction of the total integrated intensity I_T that is consistent with the thickness ratio of 80 nm of the $\mu\text{c-Si}$ layer to the total thickness of the silicon film.

The XRD results show that the HWCVD a-Si:H have narrow FSP linewidth, consistent with protocrystalline silicon. This effect is enhanced if a $\mu\text{c-Si}$ n-type template is present. Therefore, the i-layers as built-in in n-i-p solar cells have an improved MRO based on the narrower FWHM [10] for i-layers grown on $\mu\text{c-Si:H}$ film. The thinner films (0.7 μm) seem to have better MRO than the thicker films (2.0 μm). In solar cells, i-layers are usually even thinner ($\sim 0.4 \mu\text{m}$).

Figure 2 shows the SAXS results from the 1-Al, 2-Al, and 3-Al films. Sample 1-Al and 2-Al show similar SAXS while 3-Al (silicon layer structure as in cells) shows a significantly larger signal at low q indicating some larger-scale scattering features. The solid lines through the data are fits based on distributions of spheres. A Porod term [12] was included to fit the 3-Al data. A size distribution for one of the

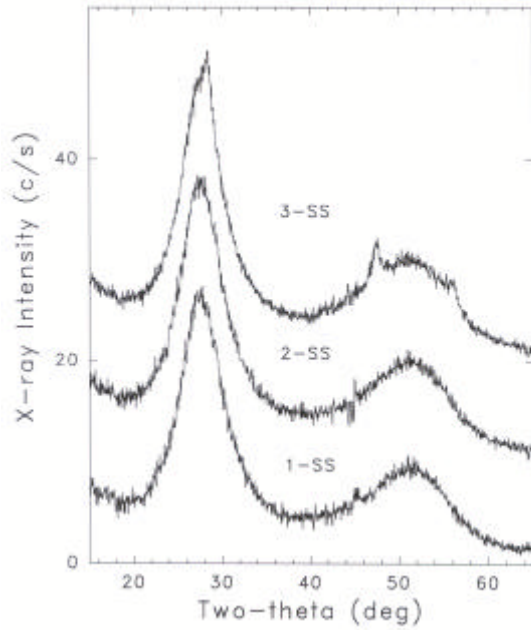


Table II. Quantitative XRD results. FWHM and P are the full-width-at-half-maximum and position of the first sharp peak of the intrinsic layer. I_T is the total integrated intensity of both a-Si:H peaks. The indicated error is the statistical uncertainty.

Sample No.	FWHM (2θ -deg)	P (2θ -deg)	I_T (deg-c/s)
1-SS	5.59 ± 0.09	27.59 ± 0.02	229
2-SS	5.55 ± 0.09	27.58 ± 0.02	236
3-SS	5.29 ± 0.11	27.64 ± 0.04	234
1-SS'	5.29 ± 0.09	27.72 ± 0.06	73
3-SS'	5.10 ± 0.09	27.82 ± 0.08	77

Fig. 1: XRD patterns from the three thick films made on SS (1-SS, 2-SS, 3-SS) after subtraction of the SS reference pattern. Sample 3-SS (on μ c-Si:H n-layer) shows evidence of the (111), (220), and (311) peaks of c-Si.

films is shown in the inset of Fig. 2. One sample (1-Al) was also measured at a 45 degrees tilt relative to the SAXS beam. A slightly reduced SAXS signal upon tilting indicates somewhat elongated scattering features aligned along the growth direction. The tilting data from 1-Al yielded an integrated intensity [12] tilt ratio $Q_N(0^\circ)/Q_N(45^\circ) = 1.6$. Since this value is larger than unity, the scattering objects cannot be spherical, but they may be thought of as ellipsoids of revolution, in which case the diameters used in the fitting will be the minor-axis diameters of the ellipsoids. The average major-to-minor axis ratio estimated from the above tilt ratio is about 2.2 based on the assumed ellipsoidal shapes. The SAXS Q_N and associated void densities are quite similar for all three films (0.11-0.15 vol.%). It is quite likely that the extra SAXS signal from 3-Al is due to the 80 nm μ c-Si layer since it is well known that SAXS from μ c-Si:H is quite strong [11]. In any case, for all three films, the void density is quite low but significantly higher than the highest density PECVD and HWCVD material where Q_N is near the detection limit of about 2×10^{22} eu/cm³ corresponding to 0.01 vol.% [12]. The size distributions of the scattering features based on fitting of spherical (or ellipsoidal) shapes are all quite similar with most probable sizes of only 2 or 3 nm. From cross-sectional TEM results (Fig. 3), we deduce that the diameter of the voids in the minor axis direction is less than 5 nm.

The flotation density results for the 3 thick films are 2.194, 2.197, and 2.219 g/cm³, respectively. These values have an uncertainty of 0.005 g/cm³, based on reproducibility in repeated measurements. The H content in the amorphous phase, C_H , can be estimated based on an established correlation [11] between density and C_H in a fully amorphous film: ρ (in g/cm³) = $2.291 - 0.0068 \cdot C_H$ (in at.%). This yields C_H values of 14 %, 14 % and 11 %, respectively. If we also correct for the maximum possible void fractions f_{\max} determined from SAXS measurements,

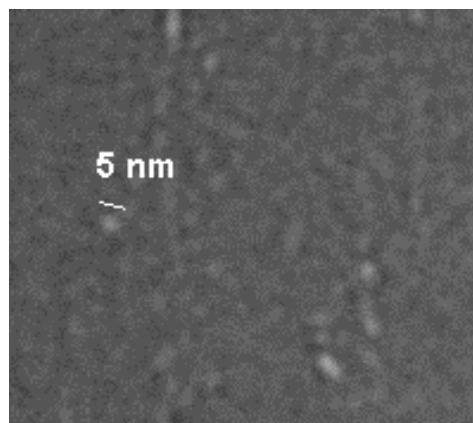
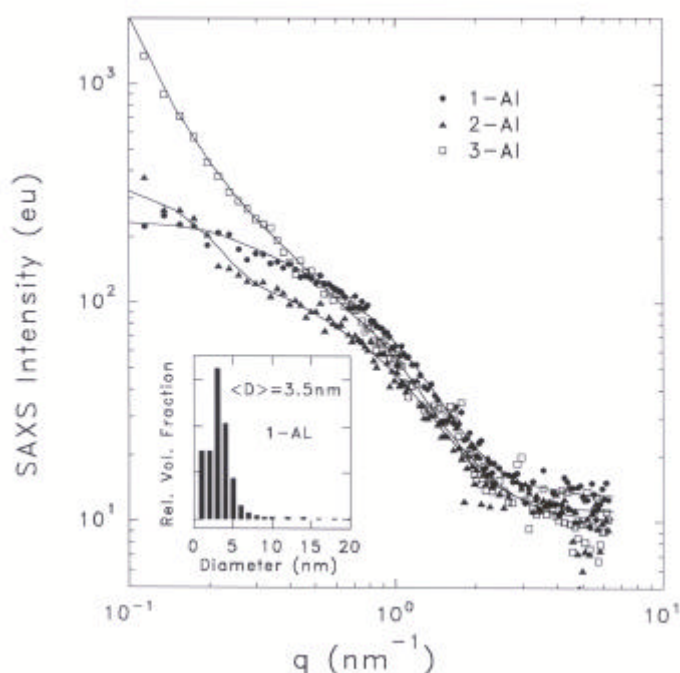


Fig. 3: Cross-sectional TEM of a protocrystalline Si film.

Fig. 2: SAXS data (symbols) and fits (lines) for the three films on Al foil. Inset shows sphere size distribution for one film.

then the flotation densities are first adjusted by $\gamma(1+0.01f_{\max})$ and then used in the above equation to yield modified C_H values. However, these corrections change C_H by less than 1% due to the small void fractions. The slightly lower C_H for 3-Al seems consistent with a slightly lower angle independent scattering (diffuse scattering), seen at the highest q values, which is controlled by the bonded H content [12].

We also determined the H content of similarly prepared layers on ϵ -Si substrates using FTIR. This H content is 12-13 %, which is quite consistent with the findings from the flotation method, considering that the different substrates induce structurally different material. The microstructure parameter R^* of these layers is 0.2-0.3, which is rather high. This indicates that a large fraction of the H is bonded at inner surfaces of voids.

SOLAR CELLS

As stated earlier [8], the open circuit voltage V_{oc} is a powerful tool in differentiating protocrystalline intrinsic layers from amorphous intrinsic layers. The n -i-p solar cells did have a high V_{oc} (0.89 V) and fill factor ($FF = 0.72$) [13]. The V_{oc} is consistent with the width of the first sharp peak FSP [10], however, this value for V_{oc} is now obtained for HWCVD cells at a substrate temperature of 250 °C rather than ~400 °C. Moreover, upon light soaking for over 1500 hours these cells show excellent stability (see Fig. 4). The changes in the FF are within 10 %.

CONCLUSION

In conclusion, we found that (i) protocrystalline silicon can be deposited by Hot-Wire CVD from pure silane without using any H_2 dilution, (ii) the deposition temperature does not need to be high and may be chosen in the same range as for PECVD or even lower, (iii) the deposition rate

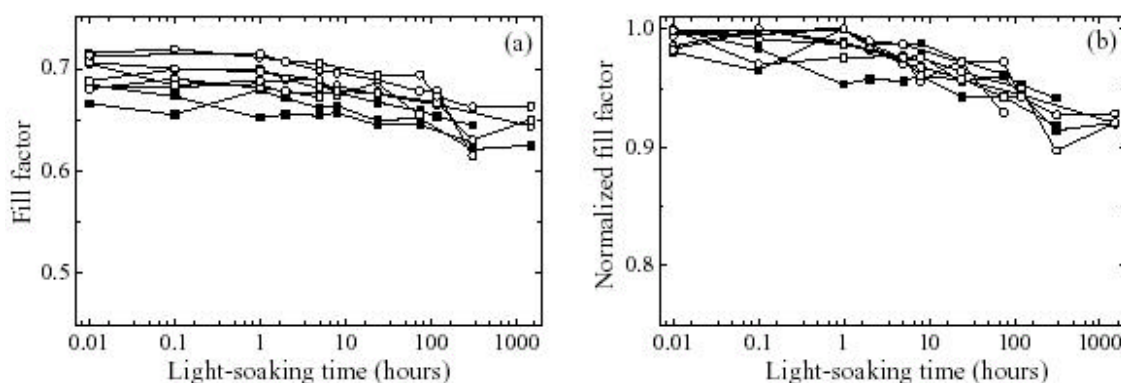


Fig. 4. (a) Fill factor and (b) normalized fill factor as a function of light-soaking time for single junction n-i-p solar cells with Hot-Wire deposited intrinsic silicon.

for protocrystalline can be much higher (~ 10 Å/s) in HWCVD than in conventional PECVD (~ 3 Å/s). Solar cells in the n-i-p configuration incorporating hot-wire deposited protocrystalline δ layers at a substrate temperature of 250 °C have demonstrated remarkable stability against light soaking, which appears to be correlated with a special void nature and enhanced medium range order.

ACKNOWLEDGEMENT

This research has benefited from the financial support from NOVEM. We are grateful to Mariëlle Rusche for ITO layers, and to Dirk Knoesen of the University of Western Cape for the TEM contributions. Support for the research at Colorado School of Mines came from NREL Subcontract No. XDJ-2-30630-27.

REFERENCES

1. A.H. Mahan, J. Carapella, B.P. Nelson, R.S. Crandall, and I. Balberg, *J. Appl. Phys.* **69** (1991) 6728.
2. H. Matsumura, *Jpn. J. Appl. Phys.* **25** (1986) L949.
3. S. Guha, K.L. Narasimhan, and S.M. Pietruszko, *J. Appl. Phys.* **52** (1981) 859.
4. D.V. Tsu, B.S. Chao, S.R. Ovshinsky, S. Guha, and J. Yang, *Appl. Phys. Lett.* **71** (1997) 1317.
5. J.H. Koh, Y. Lee, H. Fujiwara, C.R. Wronski, and R.W. Collins, *Appl. Phys. Lett.* **73** (1998) 1526.
6. R.W. Collins and A.S. Ferlauto, *Current Opinion in Solid State and Materials Science*, Vol. **6/5** (2002) 425.
7. A.H. Mahan, D.L. Williamson, and T.E. Furtak, *Mater. Res. Soc. Symp. Proc.* **467** (1997) 657.
8. S. Guha, J. Yang, D.L. Williamson, Y. Lubianiker, J.D. Cohen, A.H. Mahan, *Appl. Phys. Lett.* **74** (1999) 1860.
9. K.F. Feenstra, R.E.I. Schropp and W.F. van der Weg, *J. Appl. Phys.* **85** (1999) 6843.
10. D.L. Williamson, *Mat. Res. Soc. Symp. Proc.* **557** (1999) 251.
11. D.L. Williamson, *Solar Energy Materials and Solar Cells* **78** (2003) 41.
12. D.L. Williamson, *Mat. Res. Soc. Symp. Proc.* **377** (1995) 251.
13. M.K. van Veen and R.E. I. Schropp, in: M. Stutzmann, J. B. Boyce, J. D. Cohen, R. W. Collins and J. Hanna (Eds.), *Mat. Res. Soc. Symp. Proc.* **664**, A11.2.1 (2001).